EARTH SURFACE PROCESSES AND LANDFORMS
Earth Surf. Process. Landforms **38**, 169–178 (2013)

Published online 11 October 2012 in Wiley Online Library
(wileyonlinelibrary.com) DOI: 10.1002/esp.3310

Recalibrating aeolian sand transport models

Douglas J. Sherman,[1] Bailiang Li,[2] Jean T. Ellis,[3]* Eugene J. Farrell,[4]† Luis Parente Maia[5] and Helena Granja[6]
[1] Department of Geography, University of Alabama, Tuscaloosa, AL, USA
[2] Department of Geography, Trent University, Peterborough, Ontario, Canada
[3] Department of Geography and Marine Science Program, University of South Carolina, Columbia, SC, USA
[4] Institute of Marine and Coastal Sciences, Rutgers – The State University of New Jersey, New Brunswick, NJ, USA
[5] Instituto de Ciências do Mar, Universidade Federal do Ceará, Fortleza, Ceará, Brazil
[6] Departamento de Ciências da Terra, Universidade do Minho, Braga, Portugal

Received 18 April 2012; Revised 8 July 2012; Accepted 17 July 2012

*Correspondence to: Jean Ellis, Department of Geography and Marine Science Program, University of South Carolina, Columbia, SC 29208, USA. E-mail: jtellis@sc.edu
†Current affiliation: School of Geography and Archaeology, National University of Ireland Galway, Ireland

ESPL
Earth Surface Processes and Landforms

ABSTRACT: A quality-controlled data set comprising measurements of aeolian sand transport rates obtained at three disparate field sites is used to evaluate six commonly employed transport rate models (those of Bagnold, Kawamura, Zingg, Owen, Hsu, and Lettau and Lettau) and to recalibrate the empirical constants in those models. Shear velocity estimates were obtained using the von Kármán constant and an apparent von Kármán parameter. Models were recalibrated using non-linear regression and non-linear regression with least-squares lines forced through axes origins. Recalibration using the apparent von Kármán parameter and forced regression reduced the empirical constants for all models. The disparity between the predictions from the different models is reduced from about an order of magnitude to about a quarter of an order of magnitude. The recalibrated Lettau and Lettau model provided the greatest statistical agreement between observed and predicted transport rates, with a coefficient of determination of 0·77. Evaluation of the results suggests that our estimations of threshold shear velocity may be too slow, causing errors in predicted transport rates.

KEYWORDS: shear velocity; initiation of motion; apparent von Kármán parameter; sand transport rate models

Introduction

All aeolian sand transport models include one or more empirical calibration coefficients based on wind-tunnel measurements or field measurements from a specific environment, or both, to obtain correspondence between measured and observed transport rates. When such models are evaluated using field-based data, it is common for the models to substantially over-predict transport rates compared to those measured. Many reasons have been offered to explain the disparity, including the impacts of a suite of environmental controls not considered in the models, such as sediment moisture content, surface slope, or vegetation. We posit that at least some of the error is attributable to the values attributed to the empirical constants in those models. Some constants have been derived from wind tunnel experiments that do not use naturally graded sands and/or rely on only a few data points, or are from experiments in specific field environments, typically with few data points. Our position is based upon previous research that has demonstrated the distinct scaling constraints on wind tunnel boundary-layer conditions so that the laboratory studies cannot replicate, for example, the effects of larger-scale turbulent structures (Sherman and Farrell, 2008). Using uniform grain sizes rather than natural sands must also introduce some degree of bias. Other effects stem from the use of environment specific calibrations where complicating factors might be present, but not explicitly described (e.g., surface slope or moisture content).

The purpose of this project was to recalibrate six transport equations using quality-controlled data obtained from three disparate field experiments. The purpose of this paper is to discuss the development of the empirical coefficients in the original models, to describe the three field experiments and the data obtained, and then to use those data to obtain new calibration coefficients for the transport rate models of Bagnold (1937), Kawamura (1951), Zingg (1953), Owen (1964), Hsu (1971), and Lettau and Lettau (1978). The new calibration coefficients are compared to the originals, and both are used in a comparison of predicted and observed transport rates. We also present comparisons of those model results using the original and recalibrated coefficients and the von Kármán constant (equal to 0·4) with predictions using an adjustable, apparent von Kármán parameter (dependent on transport rate) and the recalibrated coefficients.

Background

The general inability of existing models to accurately predict wind-blown sand transport rates has been widely recognized and lamented (Horikawa *et al.*, 1986; Sherman *et al.*, 1998; Dong *et al.*, 2003; Liu *et al.*, 2006; Sherman and Li, 2011). Several reasons for the disparity between model predictions and prototype observations have been offered. First, most of the models have been developed to predict transport rates for clean and dry sand grains of uniform size and composition.

This is especially the case for models calibrated in carefully controlled wind tunnel experiments. Models calibrated using field data may not be broadly representative of typical transport conditions in other environments, unless careful accounting of local complicating conditions has been included in the models. This has not been the case for the models we consider, where such complications can only have been accounted for in the derivation of the empirical constants that correct their predictions to match measurements. One result is that, even though the general physics of the models are approximately the same, the models produce greatly different predictions of transport rates for identical environmental conditions. As an example, in Figure 1, we depict the relationships between shear velocity and predicted sand transport rates for each of the models we consider in this paper, assuming a dry, uniform sand grain size of 0·25 mm. The results vary substantially across the range of transport rates predicted by the different models. At a shear velocity of $0{\cdot}50\,\mathrm{m\,s^{-1}}$, the degree of variability approaches an order of magnitude, for example.

Many specific reasons have been offered to account for the relatively poor agreement between transport rates predicted by various models and those observed in the prototype. As noted earlier, the most frequently invoked explanations concern the use of idealized models to predict transport rates for complicated field settings (e.g. Gares, 1988; Sherman and Hotta, 1990; Bauer *et al.*, 2009; Sherman and Li, 2011). Complications arise when there is a departure from 'ideal' conditions, such as the presence of moisture (Belly, 1964; McKenna Neuman and Nickling, 1989; Namikas and Sherman, 1995; Corneilis and Gabriels, 2003), surface crusting (Leys and Eldridge, 1991; Rice and McEwan, 2001; Langston and McKenna Neuman, 2005), various fetch lengths (Nordstrom and Jackson, 1992; Jackson and Cooper, 1999; Bauer and Davidson-Arnott, 2003; Dong *et al.*, 2003; Delgado-Fernandez, 2010), local slope effects (Iversen and Rasmussen, 1999; White and Tsaor, 1998; Hesp *et al.*, 2005), unsteadiness in the wind field (Stout and Zobeck, 1997; Schonfeldt, 2004; Wiggs *et al.*, 2004; Davidson-Arnott and Bauer, 2009), variability in the saltation system (Bauer *et al.*, 1996; Gares *et al.*, 1996; Davidson-Arnott *et al.*, 1997; Baas and Sherman, 2005; Jackson *et al.*, 2006; Ellis *et al.*, 2012) or modification of the transport system caused by the presence of vegetation (Hesp, 1981; Niedoroda *et al.*, 1991; Lancaster and Baas, 1998; Arens *et al.*, 2001; Kuriyama *et al.*, 2005), among other factors (cf. review by Nickling and McKenna Neuman, 2009; or Ellis and Sherman, in press). Alternatively, errors in prediction can arise from improper field or analytical methodologies (e.g. Bauer *et al.*, 1992; or Ellis *et al.*, 2009) or the difficulty in obtaining accurate estimates of quantities, such as shear velocity, that must be derived from other measurements (e.g. Bauer *et al.*, 1992; Wiggs, 1993; Dong *et al.*, 2003; Namikas *et al.*, 2003). If it is reasonable to assume that at least part of the error associated with the predictions of transport models is attributable to some or all of the complications that we recognize, then it is also reasonable to assume that measurements made under near-ideal conditions should produce close matches between observations and predictions of sand transport rates. It is also reasonable to expect that the empirical constants developed for the several transport rate models and tuned to relatively small data sets might not be appropriate for general application.

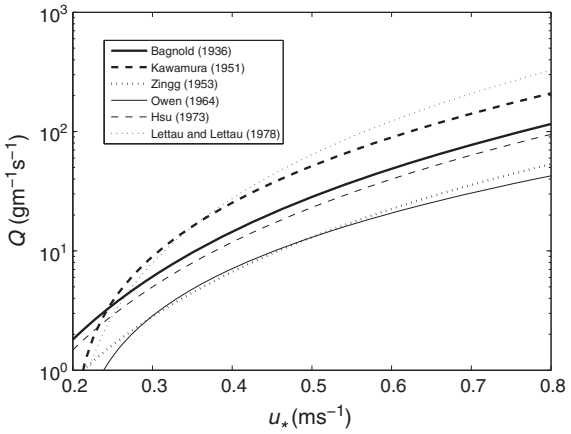

Figure 1. Comparison of transport rate predictions for the six models recalibrated herein, assuming 0·25 mm diameter sand.

It has been common practice to estimate shear velocity, u_*, using measured velocity profiles and the law of the wall, so that $u_* = \kappa m$, where κ is the von Kármán constant ($\kappa = 0{\cdot}4$) and m is the slope of the near-surface velocity profile. It has been recently demonstrated (Li *et al.*, 2010) that as aeolian sand transport rates, q, increase, the von Kármán constant appears to decrease. The variable κ has been redefined as the apparent von Kármán parameter, κ_a (Wright and Parker, 2004). Based on field experiments, Li *et al.* (2010) found the relationship $\kappa_a = -3{\cdot}03q + 0{\cdot}40$ (where units of q are in $\mathrm{kg\,m^{-1}\,s^{-1}}$). In this study we will recalibrate transport rate models using estimates of shear velocity found using κ and κ_a.

It is from these latter perspectives that we review the development of several of the most common, shear-velocity based, aeolian sand transport models, describe a series of field experiments, use data from those experiments to recalibrate the models, and then assess the results of the exercise. In order to approximate ideal transport conditions, the data sets were obtained from long fetch, minimal slope, unvegetated, dry (or nearly dry) surfaces. The results were screened to eliminate cases when the transport rates were quite small or when there was significant sediment moisture present. Details of the criteria used are discussed later.

Six aeolian transport models

Most aeolian transport models are developed from a physics/mechanical perspective using either wind velocity or wind shear velocity. Wind velocity models (O'Brien and Rindlaub, 1937; Dong *et al.*, 2003; Leenders *et al.*, 2011) offer several advantages over shear velocity models. It is easier to measure wind speed than to obtain and analyze wind profiles or Reynolds stress data to estimate shear velocity. There are, however, issues associated with wind speed models. Because wind speed is not constant with elevation near the sand surface, results from such analyses are comparable only when elevations can be standardized. Further, an elevation-specific drag coefficient should also be specified. Drag coefficients vary with fluid velocity (e.g. McEwan and Willetts, 1993), so these can only be approximations for elevation or speed. Further, drag coefficients will also vary with surface roughness characteristics (Vugts and Cannemeijer, 1981), so it is possible to have similar shear velocities with dissimilar wind speeds, or dissimilar shear velocities with similar wind speeds. These effects are typically constrained by the empirical constants in wind speed models. Shear velocity models, however, suffer from neither of these issues. There are, however, issues of appropriate averaging intervals for shear velocity estimation (Namikas *et al.*, 2003), and there has been debate concerning the appropriate exponent to be used in shear velocity-based models (e.g. Ungar and Haff, 1987; Sarre, 1988; Davidson-Arnott and Bauer, 2009, Ho *et al.*, 2011; Sherman and Li, 2011). Despite these issues, most applications use one or more

of the shear velocity cubed models that we describe later, in chronological order.

Bagnold (1937)
Bagnold first presented his model in 1937:

$$q = C_B\left(\frac{\rho}{g}\right)u_*^3\left(\frac{d}{D}\right)^{1/2} \quad (1)$$

where ρ is fluid density, g is acceleration due to gravity, d is median grain size, u_* is shear velocity (he used $V'_@$ instead of u_*), D is reference grain diameter, and C_B is Bagnold's empirical coefficient (subscripts are used to distinguish the different values of C used by the various models); the latter two parameters are discussed later. While Bagnold introduced Equation 1 in his 1937 paper, critical details outlining the calibration and experiments are discussed in his 1936 paper. The experiments were conducted in a 0·3 m wide by 0·3 m high × 10 m long wind tunnel. The tunnel had the capability to receive sand through its mouth by a stream of sand, but the details of this system, such as the flow rate, are not presented. Wind was measured with a pitot tube and sand transport was determined using 10 balances equally distributed throughout the tunnel. Bagnold approximated that total transport comprises one-quarter surface creep and the remaining saltation. Consequently, he assumed that 75% of sand movement exits the tunnel. Bagnold (1936) presented six runs with shear velocities that ranged from $u_* = 0{\cdot}19$–$0{\cdot}88\,\mathrm{m\,s^{-1}}$. Sand, ranging in size from 0·18 mm to 0·30 mm, was spread evenly on the tunnel surface. Transport rates ranged 0·042–0·122 $\mathrm{kg\,m^{-1}\,s^{-1}}$. Bagnold's 1937 paper reports the empirical coefficient value of C_B as 1·5 for uniform sand and 2·8 for sands with a wide range of sizes. Bagnold (1941) also reports C_B equivalent to 1·8 for naturally graded sand, typically found on dunes. Additionally, his 1937 paper reports D, the mean standard sand diameter as 0·24 mm. In Bagnold (1941) it is reported as $D = 0{\cdot}25$ mm, which is the value typically used in modern literature (e.g. Dong *et al.*, 2003; Nickling and McKenna Neuman, 2009; Ellis and Sherman, in press) and for the rest of this paper.

Kawamura (1951)
Kawamura (1951) relates mass transport to shear velocity using:

$$q = C_K\left(\frac{\rho}{g}\right)(u_* - u_{*t})(u_* + u_{*t})^2 \quad (2)$$

where u_{*t} is threshold shear velocity and $C_K = 2{\cdot}78$. Kawamura conducted both laboratory- and field-based experiments, however, it is unclear, perhaps because we are using a translation of the manuscript from its original form in Japanese, whether Equation 2 was formulated using both data sets or exclusively the former. However, the parameterization of $C_K = 2{\cdot}78$ is based only upon laboratory experiments: therefore, this discussion will focus only on the details of the wind tunnel experiments presented by Kawamura (1951). In the 1951 study he used a tunnel measuring 0·05 m wide by 0·80 m high and 1·5 m long to determine q. The wind tunnel sand was collected from a beach with a mean grain size of 0·248 mm; all experiments used the same sands. Sand transport was determined by measuring the weight of sand deposited in cylinders installed flush with the surface that measured 4·0 mm (inside diameter) and placed 0·25 m apart. The author discussed that erosion occurred in the upwind portion of the tunnel, which exposed the cylinders and disrupted flow. Wind was measured in the tunnel at 0·30 m above the surface and shear velocity was calculated by multiplying the single point wind speed by 0·0488. Thirteen coincident measurements of q and wind speed (converted to u_*) are presented in his figure 11 with values ranging up to approximately $0{\cdot}425\,\mathrm{kg\,m^{-1}\,s^{-1}}$ and from approximately 2·5–10·5 $\mathrm{m\,s^{-1}}$, respectively. He also estimated u_{*t} equivalent to $2{\cdot}34\,\mathrm{m\,s^{-1}}$ when wind velocity equals $4{\cdot}8\,\mathrm{m\,s^{-1}}$ at 0·30 m above the bed in the wind tunnel.

Zingg (1953)
Zingg employed a portable wind tunnel 17·1 m long by $0{\cdot}91\,\mathrm{m^2}$ (c.f. Zingg and Chepil, 1950) to support the formulation of his transport model. The wind tunnel comprised multiple 0·46 m wide trays located on center, and on the bed of the tunnel, with scales beneath. Five sizes of quartz sand were considered: 0·20, 0·275, 0·36, 0·505, and 0·715 mm. Wind velocity profiles were measured at four locations along the spanwise distance of the tunnel to determine that the growth of the boundary layer is proportional to the four-fifth power of the wind tunnel length. In the paper that introduced the wind tunnel, Zingg and Chepil (1950) noted that the first third spanwise length should not be used for measurement. Shear stress (τ_0) was measured directly using a 'shear tray' (Zingg, 1953). Transport was also measured using 'dust samplers' (Zingg, 1953), which were adapted from commercial vacuum cleaners and co-located with impact tubes that recorded pressure to determine the rate of the fluid flow. Zingg (1953) considered 43 tests, each having a 120 second duration, using the five different sand sizes and winds sampled at multiple elevations (cf. Zingg, 1953, table 3). His model:

$$q = C_Z\left(\frac{d}{D}\right)^{3/4}\frac{\rho}{g}\left(\frac{\tau_0}{\rho}\right)^{3/2} \quad (3)$$

is derived from multiple regression analysis using a power function with a correlation coefficient of 0·977 when C_Z is 0·83.

Zingg (1953) mentions that the size and shape of the wind tunnel and the turbulent boundary layer depth affects the tunnel-measured q values.

Owen (1964)
Owen (1964) formulated his model:

$$q = \left(0.25 + \frac{w_s}{3u_*}\right)\left(1 - \frac{u_{*t}^2}{u_*^2}\right)\left(\frac{\rho u_*^3}{g}\right) \quad (4)$$

where w_s is fall velocity, by considering the following two hypotheses related to saltation: (1) saltation creates aerodynamic roughness and that roughness is proportional to the saltation layer thickness; and (2) shear stress governs the concentration of saltation. This model is only applicable when w_s/u_* is small: however, the author does not quantitatively define this limitation other than noting that fine grains have large fractional values. Owen (1964) employed data from Bagnold (1941) and Zingg (1953) for grain sizes of 0·20, 0·275, 0·505, 0·715 mm to determine that the relationship between the ordinate of $\frac{qg}{\rho u_*^3}\left(1 - \frac{u_{*t}^2}{u_*^2}\right)$ and w_s/u_*, which fall according to the line $\frac{qg}{\rho u_*^3}\left(1 - \frac{u_{*t}^2}{u_*^2}\right) = 0.25 + \frac{1}{3}w_s/u_*$. Chen and Fryrear (2001) parameterize w_s using different-sized spheres:

$$w_s = -0.775352 + 4.52645d^{1/2} \quad (5)$$

where w_s is in $\mathrm{m\,s^{-1}}$ and d is in millimeters. This relationship was derived from their table 1 (Chen and Fryrear, 2001, p. 368) and was used here to solve Equation 4. The relationship described by Equation 5 is good only for sand-sized particles.

Hsu (1971)

Hsu formulated his transport model based on a 'special Froude number' (Hsu, 1971, 1973):

$$q = C_{\mathrm{H}}\left(\frac{u_*}{(gD)^{1/2}}\right)^3 \tag{6}$$

Hsu (1971) amalgamated data from seven previously published laboratory- and field-based data sets [Bagnold, 1936; O'Brien and Rindlaub, 1937; Zingg, 1941 (sic, as referenced in Hsu, 1971, 1973); Kawamura, 1951; Horikawa and Shen, 1960; Belly, 1962; Kadib, 1963, 1964] to determine his dimensional transport coefficient, C_{H}, which has the same units as q. Hsu indicates that the seven datasets are all from Kadib (1965); however, a review of Kadib (1965) reveals potential inconsistencies. Kadib (1965) reports data from Bagnold, O'Brien and Rindlaub, Kawamura, Zingg (1953 – not 1941), and his own studies. Hsu determined the best-fit line relating mean grain size and the transport coefficient has a correlation coefficient of 0·88 and is:

$$\ln\left(C_{\mathrm{H}}\cdot 10^4\right) = -0.47 + 4.97d \tag{7}$$

where d is in millimeters and C_{H} is in $\mathrm{g\,cm^{-1}\,s^{-1}}$. Mean grain size for the set of seven studies ranges from approximately 0·15 to 1·0 mm and C_{H} ranges from approximately –0·7 to $175\times10^{-4}\,\mathrm{g\,cm^{-1}\,s^{-1}}$ [values extracted from Hsu (1971, Figure 3)]. Hsu concludes his 1971 paper by indicating that the correlation coefficient could be improved with additional field-based transport data. Hsu's (1973) protocol for using Equation 6 is to deploy an anemometer at one elevation above the bed to obtain wind velocity to use in the law of the wall equation to estimate u_*:

$$\frac{u_z}{u_*} = \frac{1}{\kappa}\ln\left(\frac{z}{z_0}\right) \tag{8}$$

where u_z is velocity at elevation z above the bed, κ is von Kármán's constant and z_0 is roughness length. Hsu suggests deploying an anemometer 2 m above the bed so researchers can estimate u_* using his Figure 2, rather than Equation 7.

Lettau and Lettau (1978)

Lettau and Lettau (1978) extended the work of Kawamura (1951), as they also included threshold shear velocity to estimate transport rate:

$$q = C''\left(\frac{\rho}{g}\right)u_*^2(u_* - u_{*t}) \tag{9}$$

where C'' depends on sand size and structure, and is determined using the following:

$$C'' = C_{\mathrm{L}}\left(\frac{d}{D}\right)^n \tag{10}$$

where C_{L} (noted in their paper as C'') is a universal coefficient for sands, equivalent to 6·7, and n is 0·5 (from Bagnold and used by Lettau and Lettau, 1978). The Lettau and Lettau model may be presented as the following, which combines Equations 9 and 10:

$$q = C_{\mathrm{L}}\left(\frac{d}{D}\right)^{1/2}\left(\frac{\rho}{g}\right)u_*^2(u_* - u_{*t}) \tag{11}$$

The goal of the Lettau and Lettau book chapter, where this model was presented, was to provide a comprehensive study on barchan dunes, mainly to determine if barchan dune migration rates could be used to approximate historical wind velocities. The authors did not discuss the derivation of their transport model in detail. A comparison between their model and those from Bagnold and Kawamura, using Belly's (1962) laboratory-based data was presented. There was greatest agreement between Equation 9 and the Belly data when $C''=6{\cdot}5$ and $u_{*t}=2{\cdot}5\,\mathrm{m\,s^{-1}}$. A field experiment conducted on the crest of a barchan dune using one anemometer placed 0·63 m above the bed was used to estimate u_{*t}. Lettau and Lettau (1978) qualitatively observed sand transport as 'nil,' 'light,' or 'strong.' They compared these visual descriptions to the 30 second averages of the anemometer readings to estimate u_{*t} as $2{\cdot}2\,\mathrm{m\,s^{-1}}$ and $C''=5{\cdot}5$; when $C''=5{\cdot}5$, $C_{\mathrm{L}}=6{\cdot}7$ (using Equation 10). Lettau and Lettau (1978) also used erosion pins (wooden rulers) to measure transport on the slipfaces of five barchans dunes with $d=0{\cdot}17$ mm to determine C_{L} values. Their experiments yielded C'' values ranging from 3·9 to 8·2 (C_{L} ranging from 4·7 to 9·9), with an average of 5·4 (average $C_{\mathrm{L}}=6{\cdot}5$). However, from these data, the authors conclude a universal coefficient of sand transport (i.e. C_{L}) equivalent to 6·7.

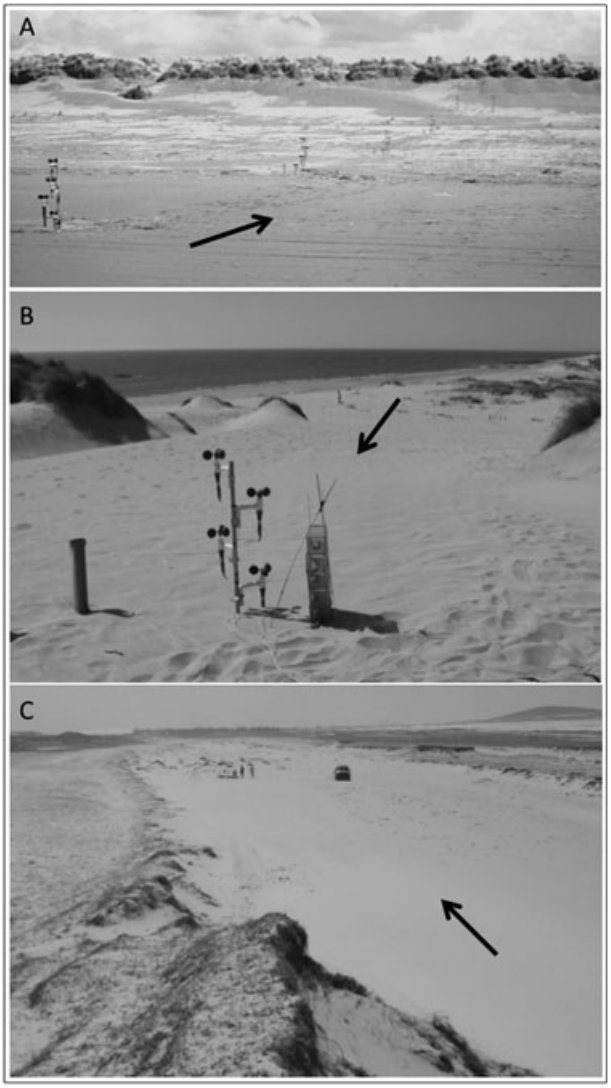

Figure 2. (A) Experimental array at Inch Spit, Ireland, with five anemometer arrays perpendicular to the shoreline. (B) Experimental array at Esposende, Portugal, with anemometer array, one set of hose traps, and one Leatherman-Rosen type trap. (C) Field site at Jericoacoara, Brazil, illustrating general experimental environment. Arrows indicate wind direction during sampling.

Study Site and Methods

Data for this project were obtained from field experiments conducted at three sites, and the data used herein are summarized in Table I. Chronologically, the experiments were at Inch Spit, Ireland (described in Sherman *et al.*, 1998), Esposende, Portugal (described in Li *et al.*, 2009), and Jericoacoara, Brazil (described in Li *et al.*, 2010). The original Inch data were obtained along the beach and back beach profile seaward of the foredune in April 1994. The Inch site is part of a morphodynamically dissipative system in Dingle Bay, on the south-western coast of Ireland (Figure 2A). Fetch distances perpendicular to the shoreline varied from 100 to almost 250 m, depending on the tide and wave conditions. The profile was surveyed daily when transport data were being obtained, and the slope averaged less than 0·05. Wind conditions were measured using five arrays of four Gill-type 3-cup anemometers installed at elevations of 0·25, 0·50, 0·75, and 1·00 m above the sand surface. The spacing of the arrays varied from 10 to 15 m, depending on the width of the dry back beach. Wind speeds were recorded at 1 Hz for data runs lasting about 1025 seconds. The heights of the anemometers were re-measured at the end of each run. Blowing sand was captured using Leatherman/Rosen type cylindrical traps with openings 40 mm wide and 450 mm high, and the bottom of the opening flush with the sand surface. The traps were co-located with anemometer arrays. Moisture samples were obtained by collecting the top 5 mm of sand by careful scraping. Samples were sealed in plastic bags. Samples for size analysis were taken from the trapped sands.

Table I. Summary of data used in this research, from the field experiments at Inch Spit, Ireland (I), Esposende, Portugal (E), and Jericoacoara, Brazil (J)

Run	T (seconds)	u_* (m s^{-1})	m	z_0 (mm)	κ_a	d (mm)	q (g m^{-1} s^{-1})
I1	1020	0·4	0·99	0·27	0·38	0·17	6·83
I2	1020	0·45	1·12	1·728	0·39	0·17	1·88
I3	1020	0·36	0·9	0·276	0·39	0·17	1·93
I4	1020	0·31	0·76	0·052	0·39	0·17	1·37
I5	1020	0·45	1·12	1·241	0·38	0·17	4·83
E1	600	0·49	1·23	0·96	0·37	0·31	8·72
E2	600	0·49	1·23	0·96	0·38	0·31	7·32
E3	900	0·41	1·03	0·45	0·39	0·31	1·61
E4	900	0·41	1·03	0·45	0·39	0·3	1·69
E5	360	0·51	1·28	1·05	0·37	0·32	8·64
E6	360	0·51	1·28	1·05	0·37	0·32	9·34
E7	900	0·41	1·03	0·36	0·35	0·35	14·4
E8	600	0·35	0·88	0·14	0·38	0·34	6·21
E9	600	0·38	0·95	0·22	0·39	0·33	3·32
E10	600	0·39	0·98	0·4	0·39	0·33	2·56
E11	900	0·32	0·8	0·25	0·4	0·28	0·32
E12	600	0·38	0·95	0·41	0·39	0·27	2·38
J1	120	0·68	1·69	3·4	0·32	0·3	31·49
J2	180	0·66	1·66	3·8	0·296	0·22	24·04
J3	180	0·71	1·78	4·19	0·264	0·22	31·45
J4	213	0·68	1·69	4·55	0·315	0·23	21·83
J5	170	0·66	1·65	2·81	0·296	0·3	26·11
J6	240	0·58	1·46	2·06	0·342	0·29	20·43
J7	240	0·56	1·41	1·81	0·353	0·28	18·03
J8	240	0·55	1·38	1·46	0·341	0·28	15·55
J9	240	0·5	1·26	1·05	0·359	0·3	15·01
J10	240	0·53	1·34	1·17	0·38	0·3	18·05
J11	240	0·54	1·35	2·02	0·357	0·25	26·31
J12	300	0·54	1·35	2·77	0·306	0·27	20·31
J13	240	0·56	1·4	0·84	0·354	0·33	22·68
J14	299	0·57	1·43	0·96	0·348	0·43	16·35
J15	240	0·57	1·44	0·9	0·341	0·44	27·31

Note: T is the duration of a sample run.

The field site at Esponsende, along the northern coast of Portugal, was near the downwind end of a parabolic dune trough (Figure 2B). Experiments were conducted in May and June, 2006. The upwind surface was flat and unobstructed, with slopes less than 0·03 in the vicinity of the traps. During the experiments the sand surface was dry and winds blew parallel to the trough with a fetch of approximately 80 m. Wind conditions were measured with one vertical array of four Gill-type, 3-cup anemometers installed at elevations of 0·25, 0·50, 0·75, and 1·00 m above the sand surface. Wind speeds were recorded at 2 Hz for periods of time ranging from 600 and 1800 seconds. Blowing sand was trapped using vertical arrays of hose-type traps. Samples for grain size analyses were obtained from sand caught in the traps.

Located on the north-eastern coast of Brazil, the Jericoacoara site was also near the downwind end of a parabolic dune trough, but at a location approximately 500 m from the shoreline (Figure 2C). The upwind surface was flat and unobstructed, with a fetch of approximately 100 m, and surface slopes less than about 0·03 in the vicinity of the traps. During the experiments, the wind blew parallel to the trough and the surface sediments were dry. Wind conditions were measured with one vertical array of four Gill-type, 3-cup anemometers installed at elevations of 0·25, 0·50, 0·75, and 1·00 m above the sand surface, or with an R.M. Young ultrasonic anemometer centered at 1 m. Both types of anemometers were sampled at 32 Hz, with record lengths that varied from 120 to 644 seconds. Sand transport rates were measured with vertical hose trap arrays (the same style used in the Esponsende study) and grain size samples were obtained from the trapped sands.

For each of the sets of experiments described, the following methods were used to obtain our results. In order to estimate shear velocity using the cup anemometer data, wind speeds were averaged over time intervals coincident with those for sand trap data. Regression analysis was used to obtain log-linear best fit lines, the slopes, m, of which were used to solve $u_* = \kappa m$. Data obtained from the ultrasonic anemometer were processed using the protocol described in Walker (2005). Shear velocity estimates were obtained from Reynolds stress estimates. Sand samples were processed in three fashions, when appropriate. Samples from the sand traps were dried and weighed to provide data for transport rate observations. Samples for grain size analysis were washed, dried, and sieved at ¼φ intervals, and the resulting data were analyzed using the method of moments. Samples for moisture content analysis were weighed, dried, and then reweighed. Weight differences were used to estimate percent water content by weight. These procedures resulted in 51 useable data sets from Inch, 13 from Esposende, and 15 from Jericoacoara.

Quality control

We reduced the number of data sets that we would use for this project by applying three important quality-control criteria. First, we selected only those wind profiles with a best-fit line r^2 exceeding 98%. This corresponds approximately to a maximum error in shear velocity of less than 10%, thus assuring a degree of confidence in using these estimates to predict sand transport rates. Second, we selected only those data for which the sand moisture content was less than 2%. Even though moisture content of this magnitude may still influence transport rates, that influence should be relatively small: 2 g water in 100 g sand produces an only slightly damp admixture. Finally, we deleted data sets where the sand transport rate, extrapolated from our measurements, was less than 0·28 g m^{-1} s^{-1}. Transport rates less than this (equivalent to

$1{\cdot}0\,\mathrm{kg\,m^{-1}\,h^{-1}}$) require that the average shear velocity exceed the threshold shear velocity only slightly, and would thus not likely represent equilibrium saltation conditions (e.g. Stout and Zobeck, 1997). As a result of these quality control steps, the number of data sets from Inch was reduced to only five, mainly because of the generally damp conditions at that field site. We retained 12 data sets from Esposende, where very slow transport rates eliminated some data. There are 15 data sets from Jericoacoara, where some data sets were eliminated with the r^2 threshold. Table I summarizes the characteristics of the 32 data sets used to recalibrate the models described earlier.

Recalibration procedures

The Bagnold (1937), Kawamura (1951), Zingg (1953), Owen (1964), Hsu (1971), and Lettau and Lettau (1978) models have empirical constants that scale their predictions of transport rates. We used these models with their original calibrations to predict transport rates with the data from the different field sites, and compared those predictions with our measured values using regression analysis (Table II). For all analyses using an estimate for threshold shear velocity, u_{*t}, that value was obtained from Bagnold's (1937) equation:

$$u_{*t} = A\left(\frac{\rho_s - \rho}{\rho} g d\right)^{1/2} \tag{12}$$

Bagnold established two values for A. When the initiation of motion is driven by fluid force alone, $A = 0{\cdot}1$. However, during active saltation, when momentum is carried to the sand surface by impacting grains, $A = 0{\cdot}085$. We used values for A that ranged from a maximum of 0·10 when the sand transport rate was about $0{\cdot}3\,\mathrm{g\,m^{-1}\,s^{-1}}$ to a minimum of 0·085 when the transport rate was $\geq 3{\cdot}0\,\mathrm{g\,m^{-1}\,s^{-1}}$. Our reasoning is that at our minimum transport rate the movement of grains will be entirely a result of fluid force. As the transport rate increases toward $3{\cdot}0\,\mathrm{g\,m^{-1}\,s^{-1}}$ the proportion of grain-borne stress will increase and the value of A will decrease to its minimum. In this case we used an exponentially decreasing A with increasing transport rate from about 0·3 to $3{\cdot}0\,\mathrm{g\,m^{-1}\,s^{-1}}$.

The statistical correspondence between observed and predicted transport rates was quite strong (Table II). All of the models produced values of r^2 between 0·75 (Zingg) and 0·80 (Kawamura and Owen). In each case $P < 0{\cdot}0001$. The root mean square error (RMSE) for the models ranged between 0·005 for the Zingg and Owen models, up to 0·027 for the Lettau and Lettau model. The differences in performance between the models are not statistically significant. These results validate the utility of our quality control protocol and the suitability of these data for recalibrating the constants in these models.

Table II. Results of regression analysis of the models with original empirical constants and using $\kappa = 0{\cdot}4$

	$q_{bagnold}$	$q_{kawamura}$	q_{zingg}	q_{owen}	q_{hsu}	q_{lettau}
$y = a + bx$						
a	0·008	0·011	0·004	0·006	0·006	0·007
b	1·87	3·45	0·87	0·92	1·53	5·24
r^2	0·78	0·80	0·75	0·80	0·79	0·79
RMSE	0·010	0·017	0·005	0·005	0·015	0·027
$y = bx$						
b	2·28	4·00	1·07	1·20	1·84	5·56
r^2	0·72	0·77	0·69	0·68	0·74	0·79
RMSE	0·011	0·018	0·006	0·006	0·015	0·027

Results for $y = a + bx$ are for normal regression analysis where a is the y-axis intercept and b is the slope of the least-squares line. RMSE is root mean square error. All results have a $P \leq 0{\cdot}0001$· Results for $y = bx$ are for the least-squares line forced through the origins of the axes.

We repeated the regression analysis with each model but omitted the constants for all but the Owen and Hsu models. The least-squares line for observed and predicted transport rates was forced through zero, and the resulting slope was the correction factor that we used to derive the new empirical constants by dividing the original constants by the correction factors. Because the Owen and Hsu models each have two constants the process was more complicated. For the Owen model, the original constants were each divided by the correction factor obtained from the regression analysis. A similar process was used for Hsu's model, except we used an average value for C_H as the original value and then repeated the other steps as described earlier. New regression statistics were obtained for each model after this phase of the recalibration.

Both phases of the recalibration were repeated with estimates of an apparent von Kármán parameter substituted for the von Kármán constant. This process requires iteration to obtain solutions for the transport models because if $q \propto u_*^3$, $u^* \propto \kappa_a$, and $\kappa_a \propto q$, then q will appear on both sides of the equations.

Results

After the first evaluation of model performance described earlier (Table II), we performed regression with the least-squares lines forced through zero of both axes. The statistical results of this recalibration exercise are summarized in Table II (note that values for probability are less than 0·0001 for all regression results reported herein, except that probability cannot be calculated for forced regression). When we force the least-squares line through zero, all of the models other than Lettau and Lettau show some degree of decrease in statistical agreement between observations and predictions. The Lettau and Lettau model performance remains at $r^2 = 0{\cdot}79$. The greatest decrease in r^2 occurred with the Owen model (from 0·80 to 0·68). The slopes of the regression lines all depart from the ideal of 1·00, although the Owen model is different by only about 8% and the Zingg model varies by about 13%. These latter models are the only among this set that under predict the observed transport rates (i.e. slopes are less than 1·00). The Kawamura and Lettau and Lettau models produce three-fold and five-fold over predictions, respectively. The RMSE values remain almost the same as those for the unforced regression.

Recalibrating the six models with $\kappa = 0{\cdot}4$ produces values of r^2 identical to the originals, but resets all of the best-fit slopes to 1·00 for the forced regression. Results of this analysis are summarized in Table III, wherein the values of b are the coefficient correction factors described earlier. The recalibrated empirical constants are presented in Table IV. In all cases the new empirical constants are less than those reported in the original papers. The smallest relative change occurs with the Zingg constant that decreases from 0·83 to 0·77. The largest absolute and relative decrease both occur with the constant in the Lettau and Lettau model that changed from 6·70 to 1·20. RMSE values decreased in all cases except for the Zingg model, with the degree of decrease paralleling the decrease in the empirical constant.

We then tested the models with their original constants using a transport-dependent, apparent von Kármán parameter (κ_a), as estimated using the relationship of Li *et al.* (2010). This method produced the best statistical results as indicated by r^2, for all of the models, although the ranking of their performances relative

Table III. Results of regression analysis of the models with recalibrated empirical constants and using $\kappa = 0{\cdot}4$

	$q_{bagnold}$	$q_{kawamura}$	q_{zingg}	q_{owen}	q_{hsu}	q_{lettau}
$y = a + bx$						
a	0·004	0·003	0·004	0·005	0·003	0·001
b	0·82	0·86	0·81	0·77	0·83	0·94
r^2	0·78	0·80	0·75	0·80	0·79	0·79
RMSE	0·004	0·004	0·003	0·003	0·005	0·005
$y = bx$						
b	1·00	1·00	1·00	1·00	1·00	1·00
r^2	0·72	0·77	0·69	0·68	0·74	0·79
RMSE	0·005	0·005	0·005	0·005	0·007	0·005

Results for $y = a + bx$ are for normal regression analysis where a is the y-axis intercept and b is the slope of the least-squares line. RMSE is root mean square error. All results have a $P \leq 0{\cdot}0001$. Results for $y = bx$ are for the least-squares line forced through the origins of the axes.

Table IV. Summary of empirical constants for the transport rate models

	Bagnold	Kawamura	Zingg	Owen	Hsu	Lettau and Lettau
C	1·8	2·78	0·83	0·25	0·33 2·57	6·7
C'_{κ}	0·79	0·70	0·77	0·21	0·28 1·28	1·20
$C'_{\kappa a}$	1·41	1·27	1·38	0·34	0·45 2·42	2·47

Note: C represents the original value for each model. C'_{κ} represents the recalibrated empirical constants using $\kappa = 0{\cdot}4$. $C'_{\kappa a}$ represents the recalibrated empirical constants using a variable κ_a.

to one another does not change (Table V). The Lettau and Lettau model is the best predictor with this approach, with $r^2 = 0{\cdot}83$, and the Zingg model still has the poorest correspondence with observations, $r^2 = 0{\cdot}77$. The overall range of values for r^2 remains relatively small, statistically. The values for RMSE are the same or smaller than those for the recalibrated results for predictions made using the von Kármán constant, with a maximum error term of only 0·005 for the Hsu and Lettau and Lettau models. However, forcing these regression lines through zero results in very large decreases in r^2. The value for the Kawamura model changes from 0·82 to 0·34, while the Lettau and Lettau value drops to 0·47. The Zingg model ($r^2 = 0{\cdot}53$) now produces the greatest correspondence between observations and predictions of blown-sand transport rates. Similarly, values for RMSE all increased with the forced regression.

Finally, we recalibrated the models using the apparent von Kármán parameter and then did the unforced and forced regression analysis (Table VI). In this case, Hsu's model, with $r^2 = 0{\cdot}63$, under performs relative to the other models which produce r^2 values ranging from 0·77 (Zingg) to 0·83 (Kawamura and Lettau and Lettau models). There is a slight improvement in RMSE, with three of the models (Bagnold, Kawamura, and Lettau and Lettau) having error terms of only 0·003. As before, the predictive powers of all models are reduced when the least-squares regression lines are forced through the origins, and all values of RMSE increased. The Lettau and Lettau model had the best statistical explanatory power with $r^2 = 0{\cdot}71$, and the Hsu model was least satisfactory with $r^2 = 0{\cdot}36$. One of the consequences of using the von Kármán parameter to estimate shear velocity is that the resulting values are less than those obtained using $\kappa = 0{\cdot}4$. Therefore all of the recalibrated constants using this approach are greater than those obtained using κ (Table IV).

Discussion

Many scholars have found large disparities between observed aeolian sand transport rates and those predicted by any of a number of the commonly used models. Such observations are often accompanied by theoretical, empirical, or methodological explanations of the errors. By careful consideration of experimental conditions and the use of quality control criteria for resulting data, we are able to compile a data set that closely approaches the ideal conditions of equilibrium saltation caused by a uniform wind field blowing across a flat, dry, unobstructed surface of unconsolidated sand grains. By this approach, we obtain the opportunity to test the performance of a set of the most commonly used transport models for wind-blown sand. Because the physics represented in the models are quite similar, they all show, in their original configurations, about the same predictive power as indicated by their values for the coefficient of determination. And from this perspective, the models were able to predict most of the variability in observed transport rates. However the values predicted for absolute transport rates varied substantially (Figure 1). This is largely a result of the large range of the empirical constants. Most of the models substantially over-predict transport rates.

Much of the over-prediction can be attributed to using the von Kármán constant (0·4) in the derivation of shear velocity estimates instead of using a transport-rate dependent, apparent von Kármán parameter. Figure 3 depicts the relationship between observed and predicted transport rates using the

Table V. Results of regression analysis of the models with original empirical constants and using a variable κ_a

	$q_{bagnold}$	$q_{kawamura}$	q_{zingg}	q_{owen}	q_{hsu}	q_{lettau}
$y = a + bx$						
a	0·009	0·012	0·005	0·006	0·007	0·011
b	0·73	0·95	0·49	0·54	0·66	1·07
r^2	0·80	0·82	0·77	0·81	0·82	0·83
RMSE	0·004	0·004	0·003	0·003	0·005	0·005
$y = bx$						
b	1·16	1·53	0·71	0·81	1·02	1·63
r^2	0·36	0·34	0·53	0·50	0·44	0·47
RMSE	0·006	0·008	0·004	0·004	0·007	0·008

Results for $y = a + bx$ are for normal regression analysis where a is the y-axis intercept and b is the slope of the least-squares line. RMSE is root mean square error. All results have a $P \leq 0{\cdot}0001$. Results for $y = bx$ are for the least-squares line forced through the origins of the axes.

Table VI. Results of regression analysis of the models with recalibrated empirical constants and using a variable κ_a

	$q_{bagnold}$	$q_{kawamura}$	q_{zingg}	q_{owen}	q_{hsu}	q_{lettau}
$y = a + bx$						
a	0·0071	0·0061	0·0072	0·0072	0·0070	0·0048
b	0·6520	0·7000	0·6470	0·6449	0·6566	0·7631
r^2	0·80	0·83	0·77	0·81	0·63	0·83
RMSE	0·003	0·003	0·004	0·003	0·005	0·003
$y = bx$						
b	1·00	1·00	1·00	1·00	1·00	1·00
r^2	0·45	0·59	0·41	0·43	0·36	0·71
RMSE	0·005	0·005	0·006	0·005	0·007	0·004

Results for $y = a + bx$ are for normal regression analysis where a is the y-axis intercept and b is the slope of the least-squares line RMSE is root mean square error. All results have a $P \leq 0{\cdot}0001$. Results for $y = bx$ are for the least-squares line forced through the origins of the axes.

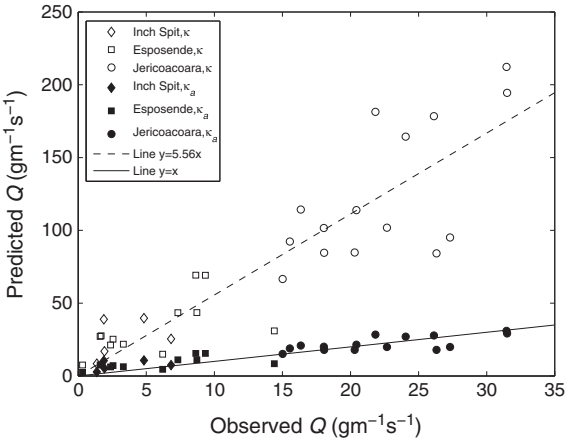

Figure 3. Comparison of the performance of the Lettau and Lettau (1978) model using its original configuration with the von Kármán constant, κ (open symbols) and after recalibration with the apparent von Kármán parameter, κ_a (closed symbols), with quality-controlled data from the three field sites: Inch Spit – diamonds; Esposende – squares; Jericoacoara – circles.

Lettau and Lettau (1978) model. The open symbols indicate data representing the original model and using the von Kármán constant. The closed symbols indicate data representing the recalibrated model and using the apparent von Kármán parameter. Both regression lines are forced through the origins of the axes. The overall improvement in model performance is apparent.

For every regression result when the least-squares line is not forced through the origins, there is a positive offset (i.e. $A > 0$). This corresponds with the over-prediction of transport rates by all of the models when q is small. It is why coefficients of determination decrease and RMSE values increase with the forced regression. Figure 4 depicts the scatter of observed and predicted transport rates for each model for observed transport rates less than $5\,g\,m^{-1}\,s^{-1}$. Note that all of the predicted transport rates exceed measured rates by a factor of about two or more. We attribute this disparity to errors in specifying values for the threshold shear velocity because we can think of no other physically plausible explanation. At transport rates less than about $5\,g\,m^{-1}\,s^{-1}$, the impact of errors in u_{*t} are much greater than they would be with faster rates. For example, consider a case when u_* is $0{\cdot}30\,m\,s^{-1}$, $d = 0{\cdot}25$ mm sands, and we are using $A = 0{\cdot}1$ (just for this example). The sand transport rate, with a recalibrated Lettau and Lettau (1978) model would be about $1{\cdot}95\,g\,m^{-1}\,s^{-1}$. If A were 0·11, as explored by Ellis and Sherman (in press), for example, then that 10% difference in u_{*t} results in predicted transport of about $1{\cdot}40\,g\,m^{-1}\,s^{-1}$, or a reduction of about 40%. This correction alone would make the predictions much closer to observations. Further, it is likely that the small moisture content in sands from some of the study sites raised threshold shear velocities at least slightly, as would be expected. In either circumstance, it is apparent that a better specification of A, or an alternative threshold model, would be useful. We did not explore alternative threshold equations (such as those of Iversen *et al.*, 1976; or Corneilis and Gabriels, 2004) because they were not used in the original models.

One result of the recalibration exercise is that the range of predictions generated by the models for standardized conditions is reduced substantially. Figure 5 is a reproduction of Figure 1 using the recalibrated models. The variability in predicted transport rates for a shear velocity of $0{\cdot}50\,m\,s^{-1}$ now spans less than a quarter of an order of magnitude rather than the near-order of magnitude of the original predictions. This implies that the selection of which transport model to use is much less important after recalibration.

Conclusions

In this paper we review the manner in which the empirical constants in six aeolian sand transport rate models were derived. We use quality-controlled data from field experiments in three diverse environments to test the efficacy of the original models and then to recalibrate those models to fit the field measurements. The recalibration was done in four ways: (1) using the von Kármán constant and an apparent von Kármán parameter to estimate shear velocity from wind speed profiles; and (2) using non-linear regression analysis and forced non-linear regression analysis to obtain the slopes of least-squares lines that were used as the bases for adjusting empirical constants. From this analysis, we can derive three conclusions:

1. All of the original transport rate models perform well for statistical prediction of transport rates when environmental conditions are close to the ideal. For the quality-controlled data set used herein, comparison of observed and predicted transport rates produced high coefficients of determination for all of the models. However RMSE values are substantial for most of the models because of the relatively steep slopes

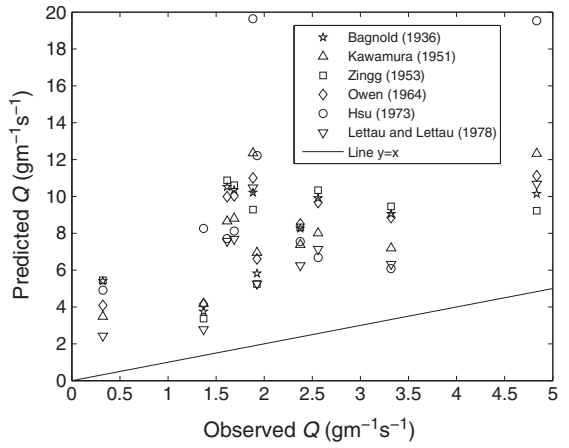

Figure 4. Comparison of observed and predicted transport rates when $q \leq 5\,g\,m^{-1}\,s^{-1}$. All of the predictions exceed observations, as indicated by the 1:1 relationship depicted by the sold line.

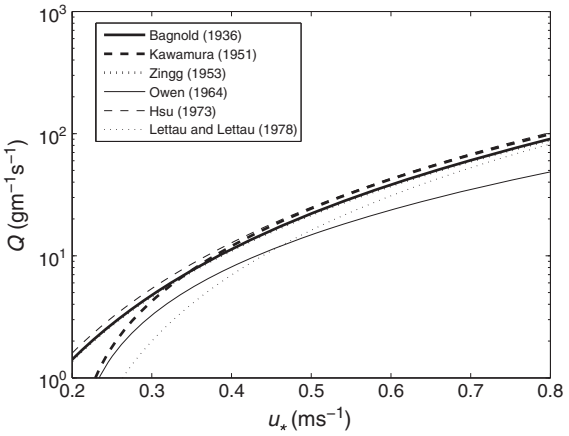

Figure 5. Comparison of transport rate predictions for the six models after their recalibration with the apparent von Kármán parameter, assuming 0·25 mm diameter sand.

of their least-squares lines. These results also support the concept that transport rates are proportional to shear velocity cubed.

2. After recalibration using the apparent von Kármán parameter and forcing the least-squares line through the origins of the axes, our analysis indicates that the Lettau and Lettau (1978) model best replicates the observed transport rates. All of the other models produce results that are significantly inferior, with the Hsu (1971) and Zingg (1953) models having the smallest r^2 and the largest RMSE.
3. There remains a need to better quantify threshold shear velocity. At transport rates less than about $3{\cdot}0\,g\,m^{-1}\,s^{-1}$, all of the models predict transport rates much greater than those observed. This is reflected in the positive offsets for results from unforced regression analysis and decreased coefficients of determination and increased RMSE for forced regression.

Our analysis indicates that performance of each of the aeolian transport rate models that we considered is improved when the models are recalibrated. These results, however, do not argue necessarily for uncritical application of any of these models. The field sites where our data were gathered were selected for the simplicity of their transport environments. Our data sets were quality controlled for moisture content and non-equilibrium transport conditions. For environments with any of the many confounding factors that we commonly encounter, there will likely still be substantial differences between measured and predicted aeolian sand transport rates. More work is necessary.

Acknowledgments—Robin Davidson-Arnott has been an inspiration to the authors, both individually and collectively. The authors thank him for his three decades of coastal and aeolian research, and for maintaining such a positive outlook even under the stresses of long periods in the field. And thanks, Robin, for the caipirinhas! Many colleagues played fundamental roles in acquiring the data for this research. For the fieldwork in Ireland, the authors enjoyed financial support from the European Community IMPACTS Project No. EV5V-CT93-0258, supervised by Julian Orford and Robert Devoy, and the US Fulbright Scholar Program to DJS. Field assistance was rendered by Cathy Delaney, Robert Devoy, Derek Jackson, John McKenna, Steve Namikas, Charles Roche, and Robert Stewart. The fieldwork in Portugal was supported by the US and Portuguese Fulbright Scholars Programs for DJS and HG. The Brazil field experiments were supported by the National Science Foundation, Geography and Regional Science Program (#0727775 and #0822482). The authors received valuable support from LABOMAR, University of Ceará, especially Robério M. Sampaio and Eduardo C. M. de Borbaand, and from colleague Walter Cox. This project is registered with the Brazilian Ministry of the Environment, Sistema de Autorização e Informação em Biodiversidade, Registration Number 18038-1. The authors appreciate the supportive comments and suggestions of the two anonymous reviewers.

References

Arens SM, Baas ACW, van Boxel JH, Kalkman C. 2001. Influence of reed stem density on foredune development. *Earth Surface Processes and Landforms* **26**: 1161–1176.

Baas ACW, Sherman DJ. 2005. Formation and behavior of aeolian streamers. *Journal of Geophysical Research* **110**: F03011.

Bagnold RA. 1936. The movement of desert sand. *Proceedings of the Royal Society of London. Series A: Mathematical and Physical Sciences* **157**: 594–620.

Bagnold RA. 1937. The transport of sand by wind. *The Geographical Journal* **89**: 409–438.

Bagnold RA. 1941. *The Physics of Blown Sand and Desert Dunes*. Chapman and Hall: London; 265.

Bauer BO, Davidson-Arnott RGD. 2003. A general framework for modeling sediment supply to coastal dunes including wind angle, beach geometry, and fetch effects. *Geomorphology* **49**: 89–108.

Bauer BO, Davidson-Arnott RGD, Hesp PA, Namikas SL, Ollerhead J, Walker IJ. 2009. Aeolian sediment transport on a beach: surface moisture, wind fetch, and mean transport. *Geomorphology* **105**: 106–116.

Bauer BO, Davidson-Arnott RGD, Nordstrom KF, Ollerhead J, Jackson NL. 1996. Indeterminacy in aeolian sediment transport across beaches. *Journal of Coastal Research* **12**: 641–653.

Bauer BO, Sherman DJ, Wolcott JF. 1992. Sources of uncertainty in shear stress and roughness length estimates derived from velocity profiles. *The Professional Geographer* **44**: 453–464.

Belly PY. 1962. *Sand movement by wind*, Monograph. Hydraulic Engineering Laboratory, Wave Research Projects, University of California: Berkeley, CA.

Belly PY. 1964. *Sand Movement by Wind*. US Army Corps of Engineers, CERC: Washington, DC.

Chen W, Fryrear DW. 2001. Aerodynamic and geometric diameter of airborne particles. *Journal of Sedimentary Research* **71**: 365–371.

Corneilis WM, Gabriels D. 2003. The effect of surface moisture on the entrainment of dune sand by wind: an evaluation of selected models. *Sedimentology* **50**: 771–790.

Corneilis WM, Gabriels D. 2004. A simple model for the prediction of the deflation threshold shear velocity of dry loose particles. *Sedimentology* **51**: 39–51.

Davidson-Arnott RGD, Bauer BO. 2009. Aeolian sediment transport on a beach: thresholds, intermittency, and high frequency variability. *Geomorphology* **105**: 117–126.

Davidson-Arnott RGD, Nielsen J, Aagaard T, Greenwood B. 1997. Alongshore and onshore aeolian sediment transport, Skallingen, Denmark. *Proceedings, Canadian Coastal Conference, Canadian Coastal Science and Engineering Association*; 463–476.

Delgado-Fernandez I. 2010. A review of the application of the fetch effect to modeling sand supply to coastal foredunes. *Aeolian Research* **2**: 61–178.

Dong Z, Liu X, Wang H, Wang X, 2003. Aeolian sand transport: a wind tunnel model. *Sedimentary Geology* **161**: 71–83.

Ellis JT, Li B, Farrell EJ, Sherman DJ. 2009. Protocols for characterizing aeolian mass-flux profiles. *Aeolian Research* **1**: 19–26.

Ellis JT, Sherman DJ. In press. Wind blown sand. In *Volume 11 of the Treatise on Geomorphology*, Lancaster N, Sherman DJ, Baas ACW (eds). Academic Press: San Diego, CA.

Ellis JT, Sherman DJ, Farrell EJ, Li, B. 2012. Temporal and spatial variability of aeolian sand transport: implications for field measurements. *Aeolian Research* **3**: 379–387.

Gares PA. 1988. Factors affecting eolian sediment transport in beach and dune environments. *Journal of Coastal Research* **SI 3**: 121–126.

Gares PA, Davidson-Arnott RGD, Bauer BO, Sherman DJ, Carter RWG, Jackson DWT, Nordstrom KF. 1996. Alongshore variations in aeolian sediment transport: Carrick Finn Strand, Ireland. *Journal of Coastal Research* **12**: 673–682.

Hesp PA. 1981. The formation of shadow dunes. *Journal of Sedimentary Petrology* **51**: 101–112.

Hesp PA, Davidson-Arnott RGD, Walker IJ, Ollerhead J. 2005. Flow dynamics over a foredune at Prince Edward Island, Canada. *Geomorphology* **65**: 71–84.

Ho TD, Valance A, Dupont P, Ould El Moctar A. 2011. Scaling laws in aeolian sand transport. *Physical Review Letters* **106**: 094501–094504.

Horikawa K, Hotta S, Kraus NC. 1986. Literature review of sand transport by wind on a dry sand surface. *Coastal Engineering* **9**: 503–526.

Hsu S-A. 1971. Wind stress criteria in eolian sand transport. *Journal of Geophysical Research* **76**: 8684–8686.

Hsu S-A. 1973. Computing eolian sand transport from shear velocity measurements. *Journal of Geology* **81**: 739–743.

Iversen JD, Pollack JB, Greeley R, White BR. 1976. Saltation threshold on Marsh: the effect of interparticle force, surface roughness, and low atmospheric density. *Icarus* **29**: 381–393.

Iversen JD, Rasmussen KR. 1999. The effect of wind speed and bed slope on sand transport. *Sedimentology* **46**: 723–731.

Jackson D, Cooper J. 1999. Beach fetch distance and aeolian sediment transport. *Sedimentology* **46**: 517–522.

Jackson NL, Sherman DJ, Hesp PA, Klein AHF, Ballasteros F, Nordstrom KF. 2006. Small-scale spatial variations in aeolian sediment transport on a fine sand beach. *Journal of Coastal Research* **39** (special issue on the proceedings of the 8th International Coastal Symposium, Santa Catarina, Brazil): 379–383.

Kadib AA. 1963. *Sand transport by wind studies with sand C (0.145 mm diameter)*. Institute of Engineers and Research Technicians Report, HEL-2-5. University of California: Berkeley, CA; 8.

Kadib AA. 1964. *Sand Movement by Wind*, Technical Memo No. 1. US Army Corps of Engineers: Washington, DC; Addendum II.

Kadib AA. 1965. *A Function of Sand Movement by Wind*, Technical Report HEL-2-12 and Dissertation. Department of Engineering, University of California: Berkeley, CA; 91.

Kawamura R. 1951. Study on Sand Movement by Wind. *Reports of Physical Sciences Research Institute of Tokyo University* **5**(3–4): 95–112 [translated from Japanese by National Aeronautic and Space Administration (NASA), Washington DC, 1972].

Kuriyama Y, Mochizuki N, Nakashima T. 2005. Influence of vegetation on aeolian sand transport rate from a backshore to a foredune at Hasaki, Japan. *Sedimentology* **52**: 1123–1132.

Lancaster N, Baas ACW. 1998. Influence of vegetation cover on sand transport by wind: field studies at Owens Lake, California. *Earth Surface Processes and Landforms* **23**: 69–82.

Langston G, McKenna Neuman C. 2005. An experimental study on the susceptibility of crusted surfaces to wind erosion: a comparison of the strength properties of biotic and salt crusts. *Geomorphology* **72**: 40–53.

Leenders JK, Sterk G, Van Boxel JH. 2011. Modeling windblown sediment transport around single vegetation elements. *Earth Surface Processes and Landforms* **36**: 1218–1229.

Lettau K, Lettau HH. 1978. Experimental and micrometeorological field studies of dune migration. In *Exploring the World's Driest Climate*, Lettau HH, Lettau K (eds). University of Wisconsin-Madison: Madison, WI; 110–147.

Leys JF, Eldridge DJ. 1991. Influence of cryptogamic crust disturbance to wind erosion on sand and loam rangeland soils. *Earth Surface Processes and Landforms* **23**: 963–974.

Li B, Granja HM, Farrell EJ, Ellis JT, Sherman DJ, 2009. Aeolian saltation at Esposende Beach, Portugal. *Journal of Coastal Research* **SI56**: 327–331.

Li B, Sherman DJ, Farrell EJ, Ellis JT. 2010. Variability of the apparent von Kármán constant during aeolian saltation. *Journal of Geophysical Research* **37**: L15404.

Liu X, Dong Z, Wang X. 2006, Wind tunnel modeling and measurements of the flux of wind-blown sand. *Journal of Arid Environments* **66**: 657–672.

McEwan IK, Willetts BB, 1993. Sand transport by wind: a review of the current conceptual model. *Geological Society, London, Special Publications* **72**: 7–16.

McKenna Neuman C, Nickling WG. 1989. A theoretical and wind tunnel investigation of the effect of capillary water on the entrainment of sediment by wind. *Canadian Journal of Soil Science* **69**: 79–96.

Namikas SL, Bauer BO, Sherman DJ. 2003. Influence of averaging on shear velocity estimates for aeolian transport modeling. *Geomorphology* **53**: 235–246.

Namikas SL, Sherman DJ. 1995. A review of the effects of surface moisture content on aeolian sand transport. In *Desert Aeolian Processes*, Tchakerian VP (ed.). Chapman and Hall: London; 269–293.

Nickling WG, McKenna Neuman C. 2009. Aeolian sediment transport. In *Geomorphology of Desert Environments*, Parson AJ, Abrahams AD (eds). Springer, Netherlands: 517–555.

Niedoroda AW, Sheppard DM, Devereaux AB. 1991. The effect of beach vegetation on aeolian sediment transport. In *Coastal Sediments*, Kraus NC, Gingrich KJ, Kriebel DL (eds). American Society of Civil Engineers: New York; 246–260.

Nordstrom K, Jackson N. 1992. Effect of source width and tidal elevation changes on aeolian transport on an estuarine beach. *Sedimentology* **39**: 769–778.

O'Brien MP, Rindlaub BD. 1937. The transportation of sand by wind. *Civil Engineering* **6**: 325–327.

Owen PR. 1964. Saltation of uniform grains in air. *Journal of Fluid Mechanics* **20**: 225–242.

Rice MA, McEwan IK. 2001. Crust strength: a wind tunnel study of the effect of impact by saltating particles on cohesive soil surfaces. *Earth Surface Processes and Landforms* **26**: 721–733.

Sarre RD. 1988. Evaluation of aeolian sand transport equations using intertidal zone measurements, Saunton Sands, England. *Sedimentology* **35**: 671–679.

Schonfeldt HJ. 2004. Establishing the threshold for intermittent aeolian sediment transport. *Meteorologische Zeitschrift* **13**: 437–444.

Sherman DJ, Farrell EF. 2008. Aerodynamic roughness lengths over movable beds: comparison of wind tunnel and field data. *Journal of Geophysical Research* **113**: F02S08.

Sherman DJ, Hotta S. 1990. Aeolian sediment transport: theory and measurement. In *Coastal Dunes: Form and Process*, Nordstrom KF, Psuty NP, Carter RWG (eds). John Wiley & Sons: Chichester; 17–37.

Sherman DJ, Jackson DWT, Namikas SL, Wang J. 1998. Wind-blown sand on beaches: an evaluation of models. *Geomorphology* **22**: 113–133.

Sherman DJ, Li B. 2011. Predicting aeolian sand transport rates: a reevaluation of models. *Aeolian Research* **3**: 371–378.

Stout JE, Zobeck TM. 1997. Intermittent saltation. *Sedimentology* **44**: 959– 970.

Ungar JE, Haff PK. 1987. Steady state saltation in air. *Sedimentology* **34**: 289–299.

Vugts HF, Cannemeijer F. 1981. Measurements of drag coefficients and roughness length at a sea–beach interface. *Journal of Applied Meteorology* **20**: 335–340.

Walker I. 2005. Physical and logistical considerations of using ultrasonic anemometers in aeolian sediment transport research. *Geomorphology* **68**: 57–76.

White B, Tsaor H. 1998. Slope effect on saltation over a climbing sand dune. *Geomorphology* **22**: 159–180.

Wiggs GFS. 1993. Desert dune dynamics and the evaluation of wind velocity: an integrated approach. In *The Dynamics and Environmental Context of Aeolian Sedimentary Systems*, Pye K (ed.). Geological Society Special Publication **72**: 37–46.

Wiggs GFS, Atherton RJ, Baird AJ. 2004. Thresholds of aeolian sand transport: establishing suitable values. *Sedimentology* **51**: 95–108.

Wright S, Parker G. 2004. Density stratification effects in sand-bed rivers. *Journal of Hydraulic Engineering* **130**: 783–795.

Zingg AW. 1953. Wind tunnel studies of the movement of sedimentary material. *Proceedings of the 5th Hydraulic Conference Bulletin*, vol. 34. Institute of Hydraulics: Iowa City, IA; 111–135.

Zingg AW, Chepil WS. 1950. Aerodynamics of wind erosion. *Agricultural Engineering* **31**: 279–282.